Supporting Information

Modulating multi-channel bistability in cyanide-bridged $\{Fe_2Fe\}$ spin-crossover coordination polymers

Xin-Feng Li[a], Hao Wang[a], Du-Yong Chen[a], Qiang Liu[b], Jingyi Xiao[b], Wen Wen[c,*], Wen-Jing Jiang[d], Liang Zhao[a], Yin-Shan Meng,[a,*] and Tao Liu[a]

[a] *State Key Laboratory of Fine Chemicals, Frontier Science Center for Smart Materials, School of Chemical Engineering, Dalian University of Technology, No.2 Linggong Road, Dalian 116024, China*

[b] *Instrumental Analysis Center, Dalian University of Technology, No.2 Linggong Road, Dalian 116024, China*

[c] *School of Chemistry & Chemical Engineering, Yantai University, No.30 Qingquan Road, Yantai 264005, China*

[d] *Fujian Science & Technology Innovation Laboratory for Optoelectronic Information of China, Fujian 350108, China*

Table S1. Crystal data and structure refinements for compound **1**.

T/K	120 K	300 K
Formula	$C_{22}H_{17}BFe_{1.5}N_{10}OS$	$C_{22}H_{17}BFe_{1.5}N_{10}OS$
CCDC	2492106	2492109
Fw	564.10	564.10
Crystal system	Monoclinic	Monoclinic
Space group	*C*2/*c*	*C*2/*c*
a (Å)	24.4993(7)	24.9757(14)
b (Å)	14.6755(4)	14.8152(10)
c (Å)	13.4219(4)	13.6874(9)
α (°)	90	90
β (°)	92.1910(10)	92.579(2)
γ (°)	90	90
V (Å^3)	4822.2(2)	5059.5(6)
Z	8	8
ρ_{calc} (g/cm^3)	1.554	1.481
F (000)	2296.0	2296.0
Reflections collected	45881	63575
Unique reflections (R_{int})	0.0532	0.0344
Goodness–of–fit on F^2	1.053	1.049
R_1 $[I>2\sigma(I)]^a$	0.0327	0.0260
wR_2 $[I>2\sigma(I)]^b$	0.0763	0.0655

$^aR_1 = \Sigma (|F_O|-|F_C|) / \Sigma |F_O|$; $^bwR_2 = [\Sigma w (|F_O|-|F_C|)^2 / \Sigma w F_O^2]^{1/2}$

Table S2. Crystal data and structure refinements for compound **2**.

T/K	120 K	300 K
Formula	$C_{23}H_{19}BFe_{1.5}N_{10}OS$	$C_{23}H_{19}BFe_{1.5}N_{10}OS$
CCDC	2492107	2492108
Fw	578.13	578.13
Crystal system	Orthorhombic	Orthorhombic
Space group	*Pbcn*	*Pbcn*
a (Å)	24.4571(9)	24.8845(9)
b (Å)	14.8845(6)	15.0561(5)
c (Å)	13.4957(5)	13.7220(5)
α (°)	90	90
β (°)	90	90
γ (°)	90	90
V (Å^3)	4912.9(3)	5141.1(3)
Z	8	8
ρ_{calc} (g/cm^3)	1.563	1.494
F (000)	2360.0	2360.0
Reflections collected	145715	109575
Unique reflections (R_{int})	0.0837	0.1089
Goodness–of–fit on F^2	1.146	1.106
R_1 $[I>2\sigma(I)]^a$	0.0488	0.0532
wR_2 $[I>2\sigma(I)]^b$	0.1143	0.1290

$^aR_1 = \Sigma (|F_O|-|F_C|) / \Sigma |F_O|$; $^bwR_2 = [\Sigma w (|F_O|-|F_C|)^2 / \Sigma w F_O^2]^{1/2}$

Table S3. Selected bond distances (Å) and angles (°) for compound **1** at 120 K.

Compound **1** $^{120\ K}$			
Fe(01)-N(006)[1]	1.9447(16)	Fe(01)-N(006)[2]	1.9447(16)
Fe(01)-N(007)	1.9970(16)	Fe(01)-N(007)[3]	1.9970(16)
Fe(01)-N(008)[3]	1.9242(15)	Fe(01)-N(008)	1.9243(15)
Fe(01)-Nav	1.9553(16)		
Fe(02)-N(004)	1.9683(16)	Fe(02)-N(00A)	1.9820(16)
Fe(02)-N(00B)	1.9774(15)	Fe(02)-C(00E)	1.9258(19)
Fe(02)-C(00J)	1.9039(19)	Fe(02)-C(00L)	1.933(2)
Fe(02)-Nav	1.9484(16)		
N(006)1-Fe(01)-N(006)[2]	180	N(006)2-Fe(01)-N(007)[3]	92.46(6)
N(006)2-Fe(01)-N(007)	87.54(6)	N(006)1-Fe(01)-N(007)	92.46(6)
N(006)1-Fe(01)-N(007)[3]	87.54(6)	N(007)3-Fe(01)-N(007)	180
N(008)3-Fe(01)-N(006)[2]	88.31(6)	N(008)-Fe(01)-N(006)[2]	91.69(6)
N(008)3-Fe(01)-N(006)[1]	91.69(6)	N(008)-Fe(01)-N(006)[1]	88.31(6)
N(008)-Fe(01)-N(007)	91.26(6)	N(008)3-Fe(01)-N(007)	88.74(6)
N(008)-Fe(01)-N(007)[3]	88.74(6)	N(008)3-Fe(01)-N(007)[3]	91.26(6)
N(008)3-Fe(01)-N(008)	180.00(9)	N(004)-Fe(02)-N(00A)	88.33(7)
N(004)-Fe(02)-N(00B)	89.85(6)	N(00B)-Fe(02)-N(00A)	87.10(6)
C(00E)-Fe(02)-N(004)	175.13(7)	C(00E)-Fe(02)-N(00A)	92.13(7)
C(00E)-Fe(02)-N(00B)	95.01(7)	C(00E)-Fe(02)-C(00L)	89.53(8)
C(00J)-Fe(02)-N(004)	90.24(7)	C(00J)-Fe(02)-N(00A)	95.98(7)
C(00J)-Fe(02)-N(00B)	176.92(7)	C(00J)-Fe(02)-C(00E)	84.89(8)
C(00J)-Fe(02)-C(00L)	85.83(8)	C(00L)-Fe(02)-N(004)	90.16(7)
C(00L)-Fe(02)-N(00A)	177.65(7)	C(00L)-Fe(02)-N(00B)	91.09(7)

[1]+X,1-Y,1/2+Z;[2]1-X,+Y,1/2-Z;[3]1-X,1-Y,1-Z

Table S4. Selected bond distances (Å) and angles (°) for compound **1** at 300 K.

Compound **1** $^{300\ K}$			
Fe(01)-N(006)^1	2.1306(13)	Fe(01)-N(006)^2	2.1306(13)
Fe(01)-N(007)^3	2.1971(14)	Fe(01)-N(007)	2.1971(14)
Fe(01)-N(00A)^3	2.0959(14)	Fe(01)-N(00A)	2.0960(14)
Fe(01)-Nav	2.1412(14)		
Fe(02)-N(004)	1.9777(13)	Fe(02)-N(005)	1.9708(13)
Fe(02)-N(008)	1.9765(13)	Fe(02)-C(00D)	1.9140(15)
Fe(02)-C(00E)	1.9018(15)	Fe(02)-C(00F)	1.9263(17)
Fe(02)-Nav	1.9445		
N(006)^1-Fe(01)-N(006)^2	180	N(006)^2-Fe(01)-N(007)^3	92.85(5)
N(006)^2-Fe(01)-N(007)	87.14(5)	N(006)1-Fe(01)-N(007)^3	87.15(5)
N(006)1-Fe(01)-N(007)	92.86(5)	N(007)-Fe(01)-N(007)^3	180
N(00A)-Fe(01)-N(006)^1	87.77(5)	N(00A)-Fe(01)-N(006)^2	92.23(5)
N(00A)^3-Fe(01)-N(006)^1	92.23(5)	N(00A)^3-Fe(01)-N(006)^2	87.77(5)
N(00A)^3-Fe(01)-N(007)	88.49(5)	N(00A)-Fe(01)-N(007)	91.51(5)
N(00A)^3-Fe(01)-N(007)^3	91.51(5)	N(00A)-Fe(01)-N(007)^3	88.49(5)
N(00A)^3-Fe(01)-N(00A)	180	N(005)-Fe(02)-N(004)	87.91(5)
N(005)-Fe(02)-N(008)	90.05(5)	N(008)-Fe(02)-N(004)	87.41(5)
C(00D)-Fe(02)-N(004)	91.74(6)	C(00D)-Fe(02)-N(005)	175.03(6)
C(00D)-Fe(02)-N(008)	94.88(6)	C(00D)-Fe(02)-C(00F)	89.88(7)
C(00E)-Fe(02)-N(004)	95.61(6)	C(00E)-Fe(02)-N(005)	91.49(6)
C(00E)-Fe(02)-N(008)	176.66(6)	C(00E)-Fe(02)-C(00D)	83.62(6)
C(00E)-Fe(02)-C(00F)	86.26(7)	C(00F)-Fe(02)-N(004)	177.65(6)
C(00F)-Fe(02)-N(005)	90.63(6)	C(00F)-Fe(02)-N(008)	90.76(7)

^{1}+X,1-Y,-1/2+Z;^{2}1-X,+Y,3/2-Z;^{3}1-X,1-Y,1-Z

Table S5. Selected bond distances (Å) and angles (°) for compound **2** at 120 K.

Compound **2** $^{120\ K}$			
Fe(01)-N(004)^1	2.015(3)	Fe(01)-N(004)	2.015(3)
Fe(01)-N(005)^2	1.960(3)	Fe(01)-N(005)^3	1.960(3)
Fe(01)-N(00D)^1	1.948(3)	Fe(01)-N(00D)	1.948(3)
Fe(01)-Nav	1.974(3)		
Fe(02)-N(007)	1.988(3)	Fe(02)-N(00A)	1.975(3)
Fe(02)-N(00B)	1.972(3)	Fe(02)-C(00F)	1.923(3)
Fe(02)-C(00I)	1.915(3)	Fe(02)-C(00J)	1.937(3)
Fe(02)-Nav	1.952(3)		
N(004)-Fe(01)-N(004)^1	180	N(005)^2-Fe(01)-N(004)^1	92.27(11)
N(005)^3-Fe(01)-N(004)	92.27(11)	N(005)^3-Fe(01)-N(004)^1	87.73(11)
N(005)^2-Fe(01)-N(004)	87.73(11)	N(005)^2-Fe(01)-N(005)^3	180
N(00D)^1-Fe(01)-N(004)^1	88.38(11)	N(00D)^1-Fe(01)-N(004)	91.62(11)
N(00D)-Fe(01)-N(004)^1	91.62(11)	N(00D)-Fe(01)-N(004)	88.38(11)
N(00D)^1-Fe(01)-N(005)^3	88.04(11)	N(00D)^1-Fe(01)-N(005)^2	91.96(11)
N(00D)-Fe(01)-N(005)^3	91.96(11)	N(00D)-Fe(01)-N(005)^2	88.04(11)
N(00D)-Fe(01)-N(00D)^1	180	N(00A)-Fe(02)-N(007)	88.04(11)
N(00B)-Fe(02)-N(007)	87.15(11)	N(00B)-Fe(02)-N(00A)	89.78(11)
C(00F)-Fe(02)-N(007)	91.88(12)	C(00F)-Fe(02)-N(00A)	90.95(12)
C(00F)-Fe(02)-N(00B)	178.77(13)	C(00F)-Fe(02)-C(00J)	90.47(14)
C(00I)-Fe(02)-N(007)	97.20(12)	C(00I)-Fe(02)-N(00A)	173.32(12)
C(00I)-Fe(02)-N(00B)	94.60(13)	C(00I)-Fe(02)-C(00F)	84.75(14)
C(00I)-Fe(02)-C(00J)	84.95(14)	C(00J)-Fe(02)-N(007)	176.95(12)
C(00J)-Fe(02)-N(00A)	89.98(13)	C(00J)-Fe(02)-N(00B)	90.52(13)

^{1}1-X,1-Y,1-Z;^{2}+X,1-Y,-1/2+Z;^{3}1-X,+Y,3/2-Z

Table S6. Selected bond distances (Å) and angles (°) for compound **2** at 300 K.

Compound **2** $^{300\ K}$			
Fe(01)-N(005)	2.213(3)	Fe(01)-N(005)[1]	2.213(3)
Fe(01)-N(00A)[1]	2.126(3)	Fe(01)-N(00A)	2.126(3)
Fe(01)-N(00B)[2]	2.161(3)	Fe(01)-N(00B)[3]	2.161(3)
Fe(01)-Nav	2.167(3)		
Fe(02)-N(004)	1.974(3)	Fe(02)-N(006)	1.980(3)
Fe(02)-N(007)	1.977(3)	Fe(02)-C(00E)	1.926(4)
Fe(02)-C(00F)	1.907(4)	Fe(02)-C(00G)	1.934(4)
Fe(02)-Nav	1.950(4)		
N(005)[1]-Fe(01)-N(005)	180	N(00A)-Fe(01)-N(005)	87.58(12)
N(00A)-Fe(01)-N(005)[1]	92.42(13)	N(00A)[1]-Fe(01)-N(005)	92.42(12)
N(00A)[1]-Fe(01)-N(005)[1]	87.58(12)	N(00A)-Fe(01)-N(00A)[1]	180.00(15)
N(00A)-Fe(01)-N(00B)[2]	87.20(13)	N(00A)-Fe(01)-N(00B)[3]	92.80(13)
N(00A)[1]-Fe(01)-N(00B)[3]	87.20(13)	N(00A)[1]-Fe(01)-N(00B)[2]	92.80(13)
N(00B)[2]-Fe(01)-N(005)	87.65(13)	N(00B)[2]-Fe(01)-N(005)[1]	92.34(13)
N(00B)[3]-Fe(01)-N(005)	92.35(13)	N(00B)[3]-Fe(01)-N(005)[1]	87.66(13)
N(00B)[2]-Fe(01)-N(00B)[3]	180	N(004)-Fe(02)-N(006)	87.28(14)
N(004)-Fe(02)-N(007)	88.21(14)	N(007)-Fe(02)-N(006)	89.55(14)
C(00E)-Fe(02)-N(004)	91.28(15)	C(00E)-Fe(02)-N(006)	177.62(16)
C(00E)-Fe(02)-N(007)	92.30(15)	C(00E)-Fe(02)-C(00G)	90.75(17)
C(00F)-Fe(02)-N(004)	96.13(15)	C(00F)-Fe(02)-N(006)	94.99(15)
C(00F)-Fe(02)-N(007)	173.86(15)	C(00F)-Fe(02)-C(00E)	83.28(17)
C(00F)-Fe(02)-C(00G)	85.53(17)	C(00G)-Fe(02)-N(004)	177.52(16)
C(00G)-Fe(02)-N(006)	90.74(16)	C(00G)-Fe(02)-N(007)	90.28(16)

[1]1-X,1-Y,1-Z;[2]+X,1-Y,-1/2+Z;[3]1-X,+Y,3/2-Z

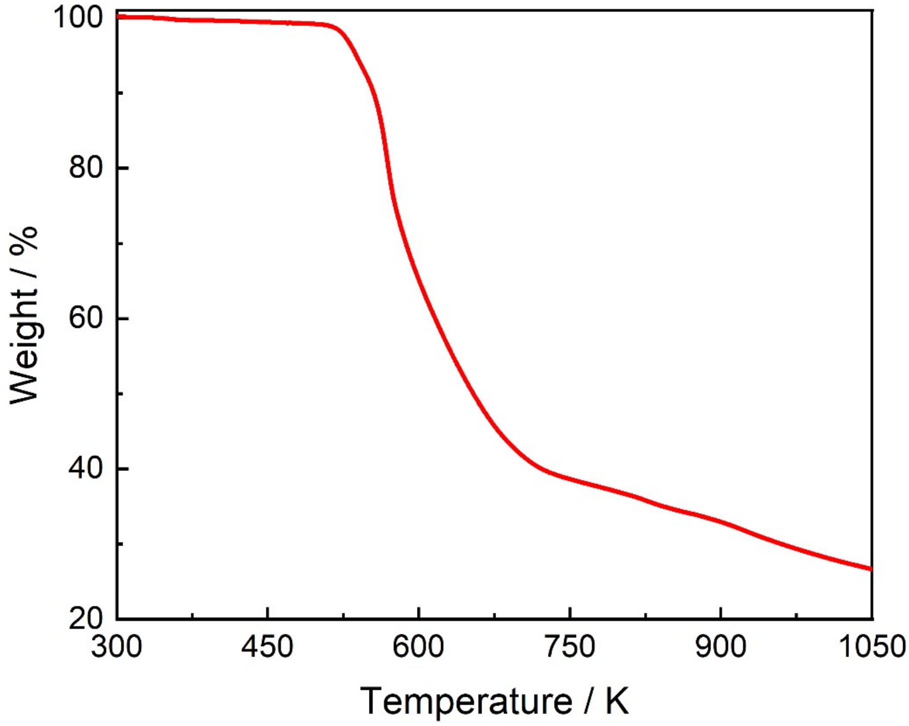

Figure S1. Thermogravimetric analysis curve of compound **1** in the nitrogen atmosphere with the sweeping rate of 10 K/min.

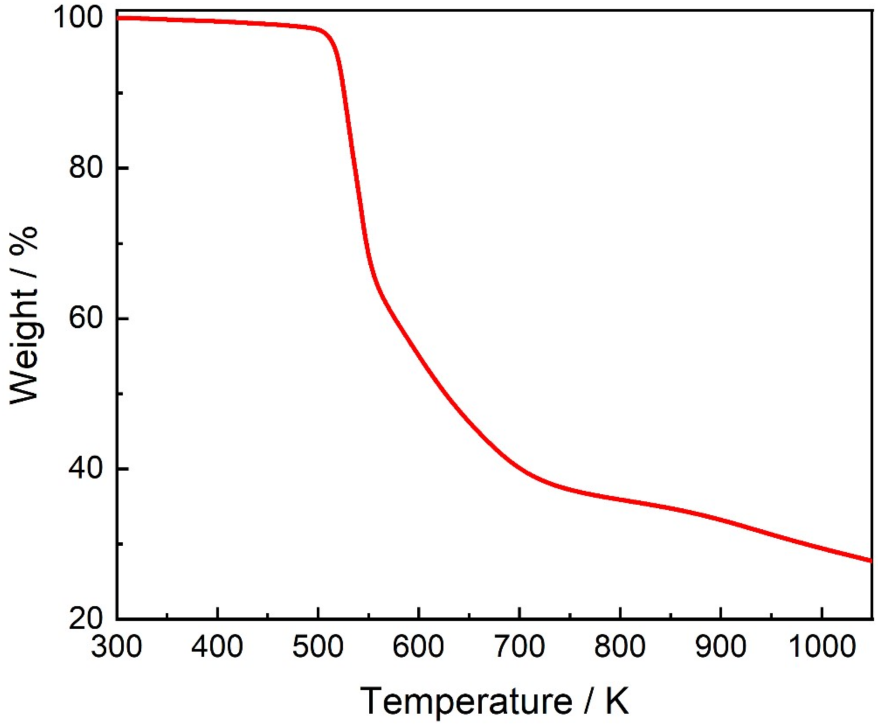

Figure S2. Thermogravimetric analysis curve of compound **2** in the nitrogen atmosphere with the sweeping rate of 10 K/min.

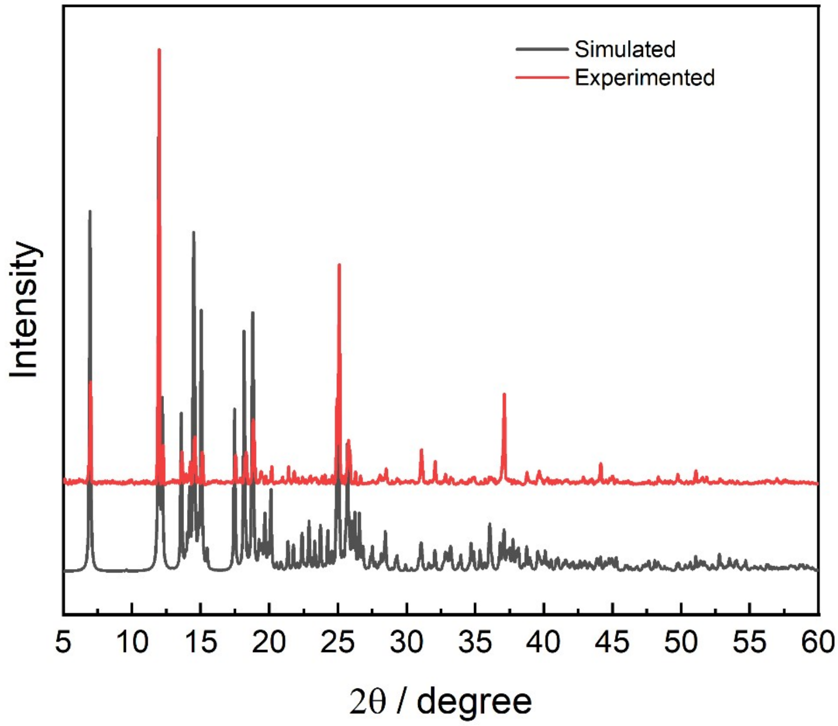

Figure S3. X-ray powder diffraction data for compound **1**. The experimental data were collected at room temperature, while the simulated data were derived from single-crystal data at 300 K.

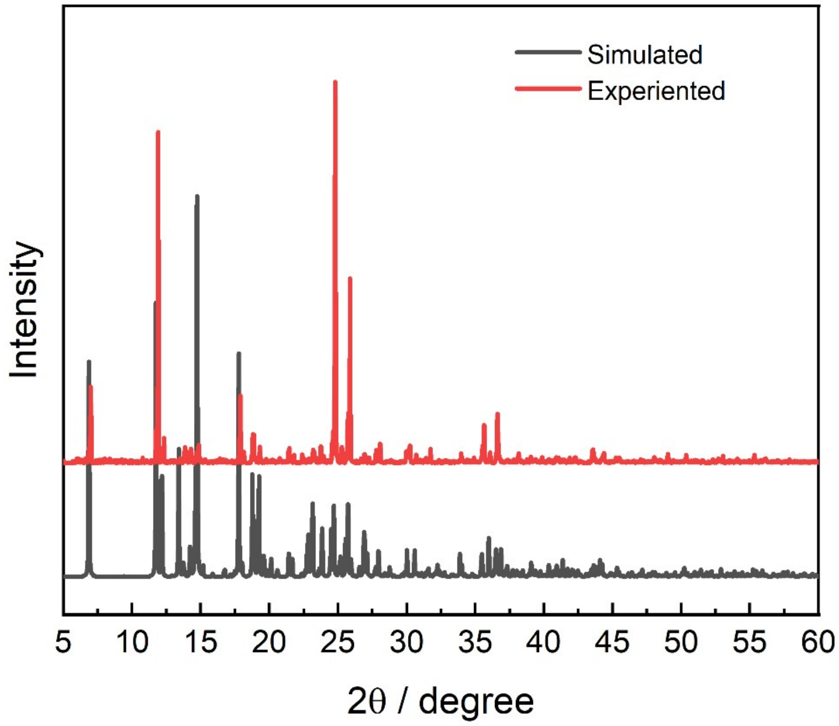

Figure S4. X-ray powder diffraction data for compound **2**. The experimental data were collected at room temperature, while the simulated data were derived from single-crystal data at 300 K.

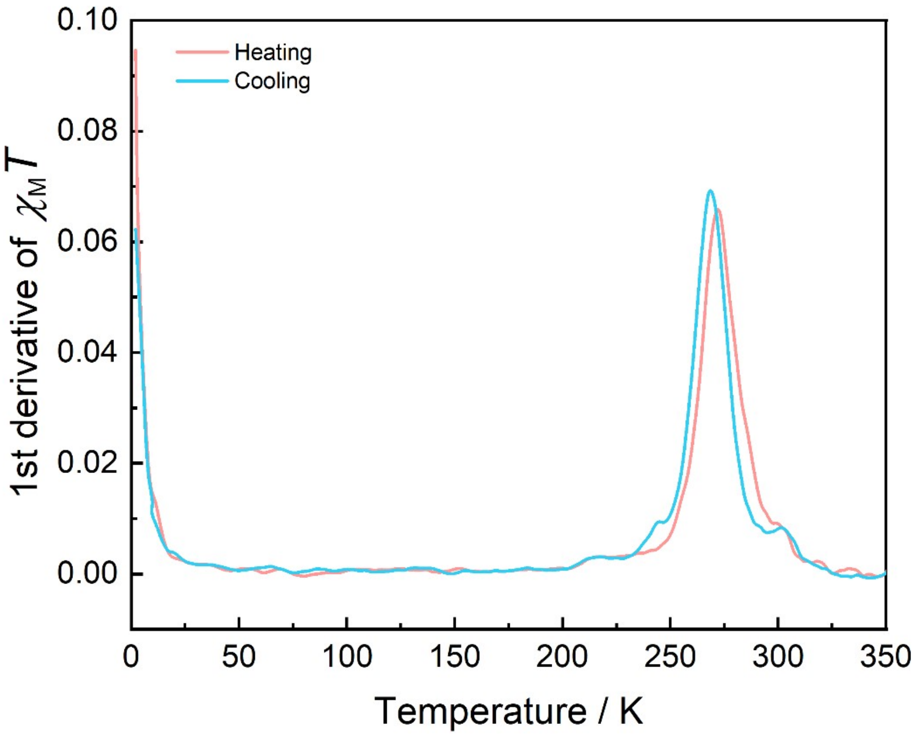

Figure S5. The 1st derivative of $\chi_M T$ plots showed the one-step spin transitions for compound **1**.

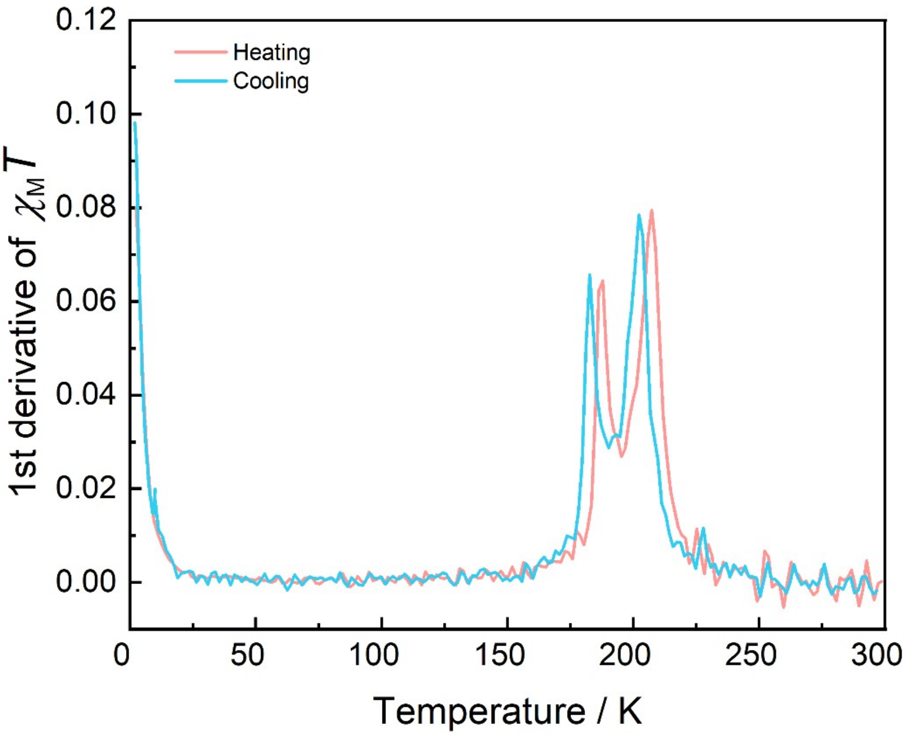

Figure S6. The 1st derivative of $\chi_M T$ plots showed the two-step spin transitions for compound **2**.

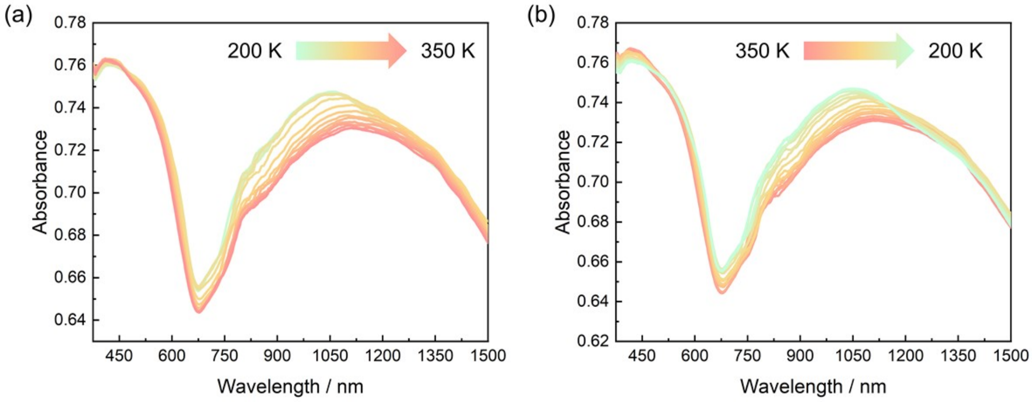

Figure S7. Temperature-dependent UV-Vis absorption spectra from 200 to 350 K for compound **1** at heating (a) and cooling (b) modes.

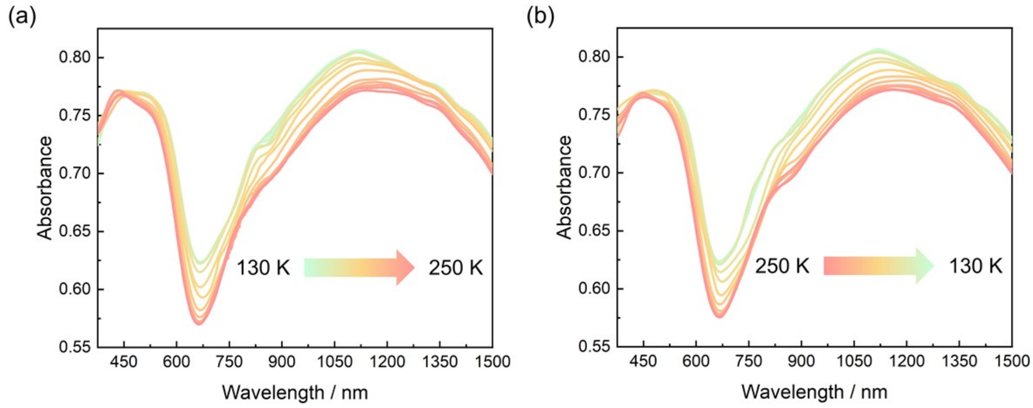

Figure S8. Temperature-dependent UV-Vis absorption spectra from 130 to 250 K for compound **2** at heating (a) and cooling (b) modes.

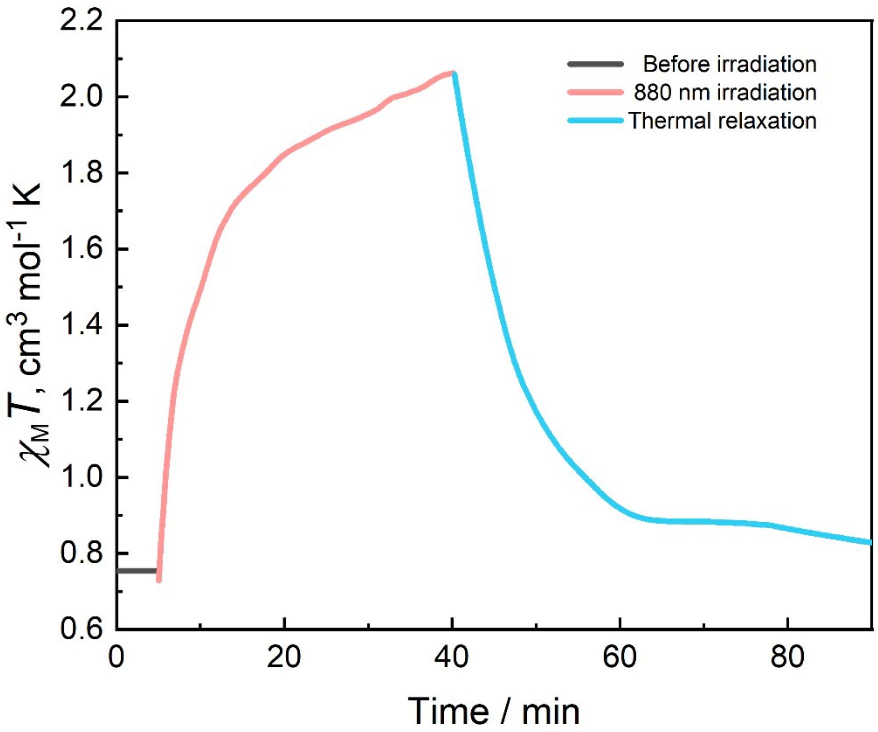

Figure S9. $\chi_M T$ vs time plots of compound **2** under successive 880-nm light irradiation and thermal relaxation process at 10 K and 1 kOe.

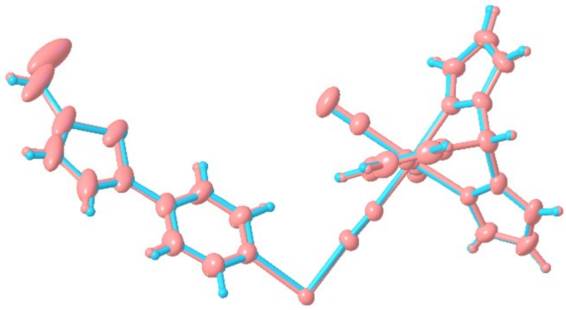

Figure S10. The overlapped diagram of compound **1** at 120 K (blue) and 300 K (pink).

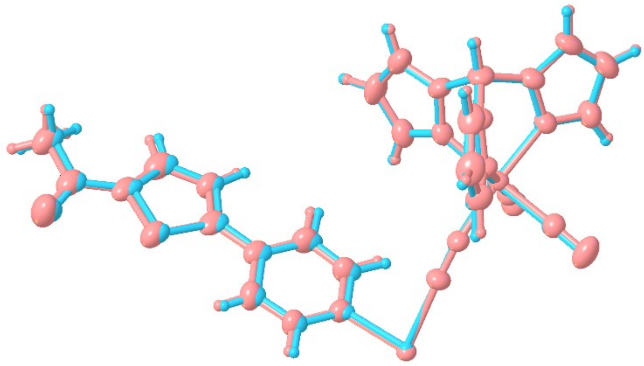

Figure S11. The overlapped diagram of compound **2** at 120 K (blue) and 300 K (pink).

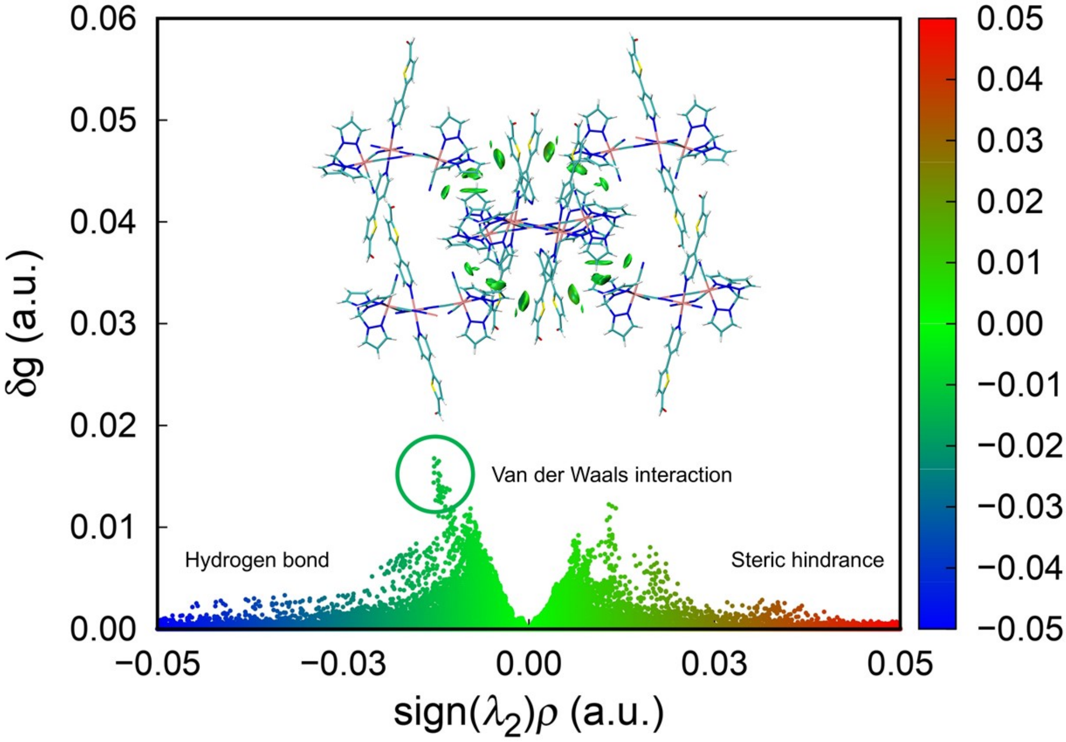

Figure S12. The distribution of the independent gradient model (IGM) isosurfaces was represented by scatter plots of sign(λ_2)ρ at 300 K for compound **1**.

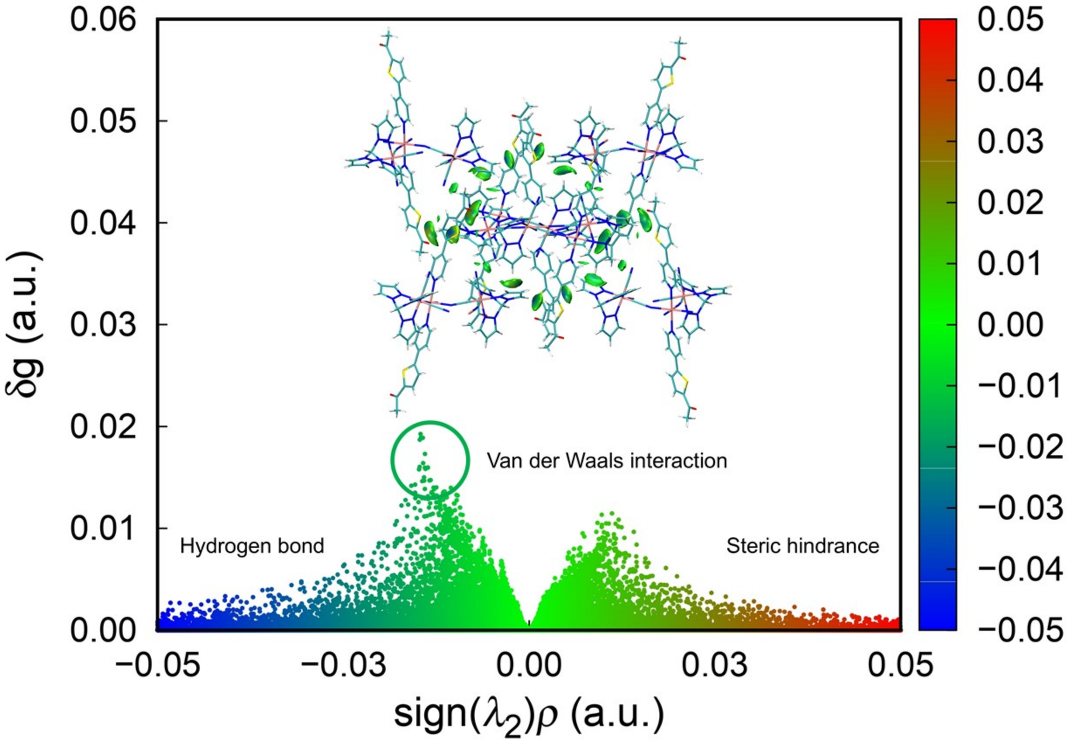

Figure S13. The distribution of the independent gradient model (IGM) isosurfaces was represented by scatter plots of sign(λ_2)ρ at 300 K for compound **2**.